Molecular hydrogen sorption capacity of *D*-shwarzites

Pavel O. Krasnov[1], Guzel S. Shkaberina[1], Alexander A. Kuzubov[2], Evgenia A. Kovaleva[2]

[1]Reshetnev Siberian State Aerospace University, Krasnoyarsk 660049, Russia
[2]Siberian Federal University, Krasnoyarsk 660041, Russia

Abstract

Schwarzites are one of the most well-known forms of nanoporous carbon. High porosity and large surface area of these materials make them promising candidates for molecular hydrogen storage. Quantum-chemical modeling showed that hydrogen weight fraction inside *D*-schwarzite structure depends on the number of atoms per unit cell that determines its size and morphology. *D*480 schwarzite has demonstrated the largest value of hydrogen sorption capacity amongst the structures considered in this work. It reaches 7.65% at the technologically acceptable values of temperature and pressure (300 K and 10 MPa). Though being lower than that required by DOE (9%), this amount can be increased by using schwarzites with larger unit cell corresponding to the larger surface area.

Keywords: carbon nanostructures; hydrogen storage; fugacity; PM6 method; dispersion interaction; Grimme correction

1. Introduction

Carbon nanostructures have been considered as promising materials for molecular hydrogen storage for more than 20 years [1-8]. Thousands of works have been published regarding carbon allotropes, namely, carbon nanotubes (CNT) [9-15], fullerenes [16-17], their metal complexes [18-26], nanoporous carbon [27-37] and other carbon structures as materials for hydrogen power engineering. Here we mainly cite the results summarized in review articles.

The main characteristic of hydrogen storage material is its molecular hydrogen sorption capacity, i.e. weight fraction of hydrogen in sorbent. The USA Department of Energy (DOE) set this parameter to be 6.5% [38] 15-20 years ago. At the moment, this value is increased up to 9.0% [39]. Carbon nanostructures were expected to fulfill this criterion due to their large surface area which is essential for gas adsorption. However, even for the same materials results obtained by different scientific groups can be in contradiction with one another [2,13-15,27]. For instance, the pioneer work of *Dillon et al.* [40] reports room-temperature H_2 sorption capacity of CNT to be 5-10% at 0.1 MPa. Still, *Hirscher et al.* [41] found it to not exceed 0.1 % under the same conditions. This discrepancy can be caused by either method of investigation (experimental or theoretical techniques implemented), experimental conditions (sample quality, impurity atoms), CNT diameter, its defectiveness etc. [1]. In general, sorption

capacity of CNT is considerably low and doesn't exceed 1% [13-15]. It can be increased when lowering the temperature down to the cryogenic values or increasing the pressure up to the hundreds bar. However, both temperature and pressure should take the extreme values to reach the capacity required by DOE, which is expensive and unreasonable for commercial use. The key issue is the low energy of hydrogen physisorption on the carbon surface (3.0-7.2 kJ/mol [1,27]). Assuming that hydrogen behaves as an ideal gas, one can briefly estimate kinetic energy of its molecules to be $^5/_2RT$ = 6.2 kJ/mol at 298 K. Practically, this means that the energy of hydrogen molecules interaction with carbon materials is comparable to the energy of their heat motion and explains low room-temperature capacity along with its increasing at cryogenic values.

The way to reinforce hydrogen bonding with carbon materials was proposed on the footing of data regarding the sorption capacity of graphite [42,43]. The main idea expressed in these works is that hydrogen adsorption should take place when either the interplanar spacing in graphite is increased or several surfaces are involved into the interaction with hydrogen increasing adsorption energy up to the value required for the efficient hydrogen storage. This can be, in principle, reached by the intercalation of some molecules into graphite structure [43]. Still, the simplest way is to use carbon structures with large (6-7.5 Å [42], 6.2-6.4 Å [43]) spacing between adjacent surfaces. Nanoporous carbon allotropes formed by sp^2 carbon polygons containing 5-8 atoms and sp^3 carbon atoms can be efficiently used for this purpose [27-37]. Experimentally obtained materials usually don't have strictly ordered structure or periodicity and consist of various fragments of other carbon forms. In general, they can be referred as the carbon foam [27,35,36]. In theoretical works, carbon foam is mainly considered as material structured in some way. For example, graphite-like fragments connected to each other by sp^3 carbon atoms [28,32] or welded carbon nanotubes [30,37] were proposed as models for the carbon foam. Schwarzites are one of the most well-known nanoporous carbon structures [44-47]. These materials are strictly periodic and consist of sp^2 carbon atoms forming hexa-, hepta- and octagons with negative Gaussian curvature corresponding to the Schwarz minimal surface. For instance, *Vanderbilt* and *Tersoff* [44] in their pioneer work predicted the C_{60} counterpart with *D* (*diamond-like*) negative surface curvature, so-called *Buckygym*, containing 168 carbon atoms. Besides that, there are also schwarzites with *P* (*primitive*) and *G* (*gyroid*) surfaces [46,47].

Here we report the results of quantum chemical investigation of molecular hydrogen sorption capacity of *D*-schwarzites containing 168, 224, 360 and 480 carbon atoms. The impacts of temperature and external hydrogen pressure and perspectives of their usage as molecular hydrogen storage materials are discussed.

2. Model and computational methods

Reference structure of schwarzite *D*168 [44] and analogously modeled structures of schwarzites *D*224, *D*360 and *D*480 (see Figure 1) were chosen for the investigation. These periodic structures

possess face-centered cubic cells with $Fd\bar{3}$ (*D*168), $R3m$ (*D*224) and $R\bar{3}m$ (*D*360 and *D*480) space symmetry groups.

First, equilibrium geometries of *D*-schwarzites unit cells were optimized. All calculations were carried out in MOPAC2016 [49] program package using semi-empirical PM6-D3 [48] method with *Grimme* [50] correction for dispersion interactions. Tables S1-S4 [Supplementary Material] show the values of corresponding translation vectors and non-equivalent atoms positions defined using FIND-SYM [51] software.

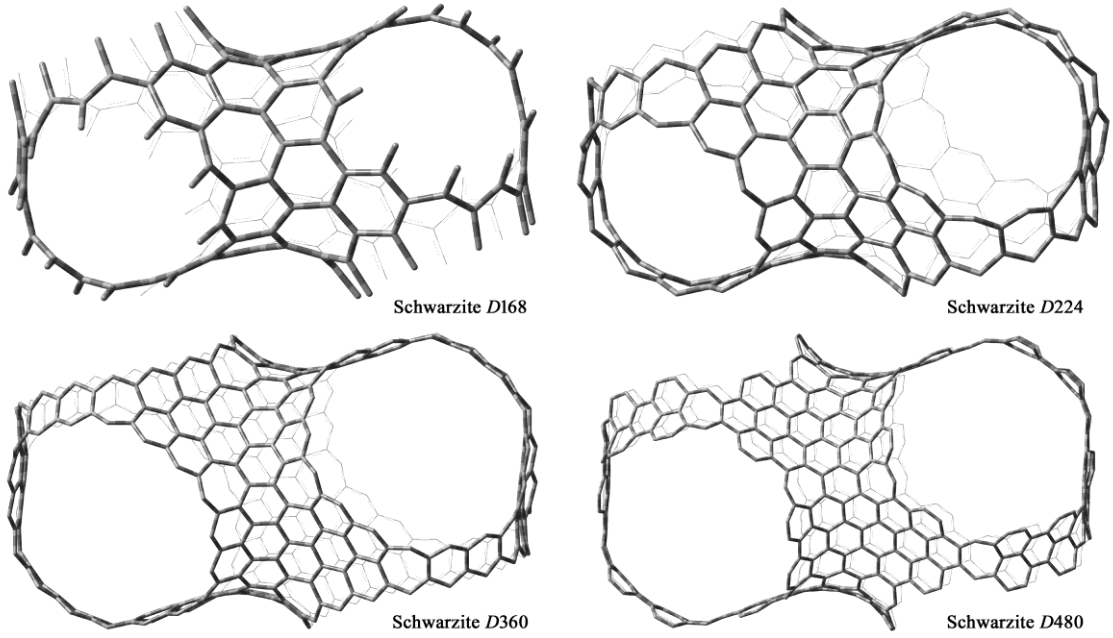

Figure 1 – Unit cells of *D*-schwarzites

Next, hydrogen molecules were placed into the unit cells (see Table 1). For each hydrogen concentration 10 different initial distributions of H_2 molecules were considered. Then, their equilibrium positions were found in the frozen carbon structure. These results correspond to the ones obtained at the ambient pressure of 1 atm. and 298 K.

Table 1 – Amount of hydrogen inside the unit cells of carbon nanostructures

Schwarzite	Number of H_2 molecules/ hydrogen weight fraction, %							
*D*168	10/0.98	20/1.95	30/2.89	40/3.82	50/4.73	60/5.62	70/6.49	80/7.35
*D*224	10/0.74	25/1.83	40/2.89	55/3.93	70/4.95	85/5.95	100/6.93	115/7.88
*D*360	40/1.82	60/2.70	80/3.57	100/4.42	120/5.26	140/6.09	160/6.90	180/7.69
*D*480	60/2.04	90/3.03	120/4.00	150/4.95	180/5.88	210/6.80	240/7.69	270/8.57

After the structural optimization, values of thermodynamic functions (heat of formation ΔH_T, entropy S_T) for the hybrid structure and its constituents were found using the second-derivative matrix

calculation and vibrational modes analysis [52] within the temperature range of 200-600 K (with the step of 10 K). Even though $\Delta H_T(H_2)$ should be zero since the molecular hydrogen is the simple substance, PM6 method results in −25,732 kcal/mol [49] at 298 K due to the parameterization features. This value similarly is not equal to zero for all other temperatures as well.

Then, hydrogen fugacity *f* needed for the given hydrogen concentration inside the carbon structure at the corresponding temperature was estimated as follows:

$$\Delta G_T = \Delta H_T\left[C_x\left(H_2\right)_n\right] - \Delta H_T\left(C_x\right) - n\Delta H_T\left(H_2\right) - T\left\{S_T\left[C_x\left(H_2\right)_n\right] - S_T\left(C_x\right) - nS_T\left(H_2\right)\right\}, \quad (1)$$

$$S_T\left(H_2\right) = S_T^0\left(H_2\right) - R\ln f, \quad (2)$$

where ΔG_T is the Gibbs energy change for the hydrogenation of carbon structure, x = 168, 224, 360 and 480 for the number of carbon atoms in the unit cell, R is the gas constant, ΔH_T and S_T are the heat of formation and entropy for the corresponding compound. ΔG_T is equal to zero for the equilibrium between free and adsorbed H_2 molecules, which allows one to define the fugacity for the given amount of hydrogen inside the schwarzite. This, in turn, gives the pressure of H_2 needed for the equilibrium at the given temperature. It should be noted that despite the fact ΔH_T and S_T calculated for the solid state correspond to the 1 atm. pressure, they still can be used in Eq. (1) due to the absence of pressure dependence. In contrast to that, hydrogen entropy $S_T(H_2)$ is strongly dependent on pressure and should be then defined according to the Eq. (2). Here, the first term in the right part of equation is the entropy at 1 atm. and given temperature, the second term is the fugacity supply to the entropy. Since there were 10 possible configurations of hydrogen distribution for each concentration, average values of ΔH_T and S_T were used for fugacity estimation.

Hydrogen gas pressure needed for the reference concentration of H_2 inside the schwarzite structure was defined using corresponding values of *f*. Fugacity is the function of pressure and temperature and can be expressed as $f = \varphi \cdot P$, where φ is the fugacity coefficient defined as [53]

$$\ln\varphi = C_1P - C_2P^2 + C_3\left[\exp\left(-P/300\right) - 1\right], \quad (3)$$

$$C_1 = \exp\left(a_1T^{1/8} + b_1\right), \quad C_2 = \exp\left(a_2T^{1/2} + b_2\right), \quad C_3 = 300\exp\left(a_3T + b_3\right). \quad (4)$$

Here a_1, b_1, a_2, b_2, a_3, b_3 are adjustable parameters (see Table 2), temperature and pressure are expressed in K and atm., respectively. These values were previously defined for the temperature range of 273-1273 K [53]. However, as the lowest temperature in this study was 200 K, nonlinear minimization of function (3) was performed using generalized reduced gradient method in the temperature range of 198-773 K with *f* and *P* values adopted from the ref. [54] (see Table 2). The comparison of *f* values obtained with different a_1, b_1, a_2, b_2, a_3, b_3 sets and experimental results (see Table S5) [Supplementary Material] showed that the newly-defined one gives much less discrepancy with experiment (0.8%) than the reference [53] parameter set (11%).

Transforming the Eq. (3) as

$$f = P\exp\left\{C_1 P - C_2 P^2 + C_3\left[\exp\left(-P/300\right)-1\right]\right\}, \quad (5)$$

one can find the sought-for values of pressure from the corresponding fugacity at given temperatures.

Table 2 – Adjustable parameters *a* and *b* for the Eq. (4)

	A_1	b_1	a_2	b_2	a_3	b_3
Ref. [53]	−3.8402	0.5410	−0.1263	−15.980	−0.11901	−5.941
Present work	−3.5607	−0.0448	−0.0317	−19.059	−0.00887	−6.526

3. Results and discussion

3.1. Interaction of H_2 molecule with π-conjugated carbon surface

The structures under investigation are characterized by the large number of atoms, which makes *ab initio* calculations computationally expensive. Semi-empirical PM6-D3 method allows treating such large systems and describes well their geometry and thermochemical parameters, especially when there are first and second period atoms only, which is exactly the case. For instance, the average discrepancy between PM6-D3 and experimental values of bond distances in hydrocarbon molecules is only 0.016 Å [49]. PM6-D3 interatomic distance in hydrogen molecule is only 0.02 Å larger than corresponding experimental value of 0.72 Å [55]. The relative error of hydrogen entropy calculated in the temperature range of 298-1500 K doesn't exceed 0.45% (see Table S6) [Supplementary Material].

Besides that, the parameters of H_2 dispersion interaction with polyatomic aromatic hydrocarbons (PAH) that can be used as the rough approximation of carbon surface are in good agreement with the ones obtained using MP2 method with large basis sets. This was proved by performing additional quantum chemical calculations of binding energies between H_2 and benzene/coronene molecules as the function of distance between their centers of mass. First, the free-standing molecules were optimized. Then, the center of Cartesian coordinate system was shifted to the center of PAH molecule and *z* axis was set to be normal to the carbon structure. H_2 molecule was then aligned along *z* axis (see Figure 2). Distance *R* between molecular centers of mass was changed with the step of 0.01 Å, and binding energy E_{int} was estimated as:

$$E_{\text{int}} = \Delta H_f\left(\text{PAH}\cdots\text{H}_2\right) - \Delta H_f\left(\text{PAH}\right) - \Delta H_f\left(\text{H}_2\right), \quad (6)$$

where each term on the right corresponds to the heat of formation for the compound in parentheses. Hydrocarbon atoms were fully frozen during the optimization while hydrogen atoms were fixed in *xy* plane and allowed to move along *z* axis. Hence, the bond distance in H_2 molecule was optimized for each *R*.

Equilibrium distance between hydrogen and benzene molecule was found to be 2.91 Å with corresponding binding energy of 3.74 kJ/mol. Reference values obtained using MP2 method with cc-pVTZ basis set and BSSE correction are 3.09 Å and 3.78 kJ/mol [56], 3.20 Å and 3.73 kJ/mol [42],

respectively (see Figure 2). Thus, dispersion interaction parameters for H_2 and C_6H_6 molecules implemented in PM6-D3 agree well with more accurate methods. Similarly, the equilibrium distance between hydrogen and coronene molecule is 2.86 Å with corresponding energy of 5.38 kJ/mol while BSSE-corrected MP2/cc-pVTZ gives 2.90 Å and 6.46 kJ/mol [42].

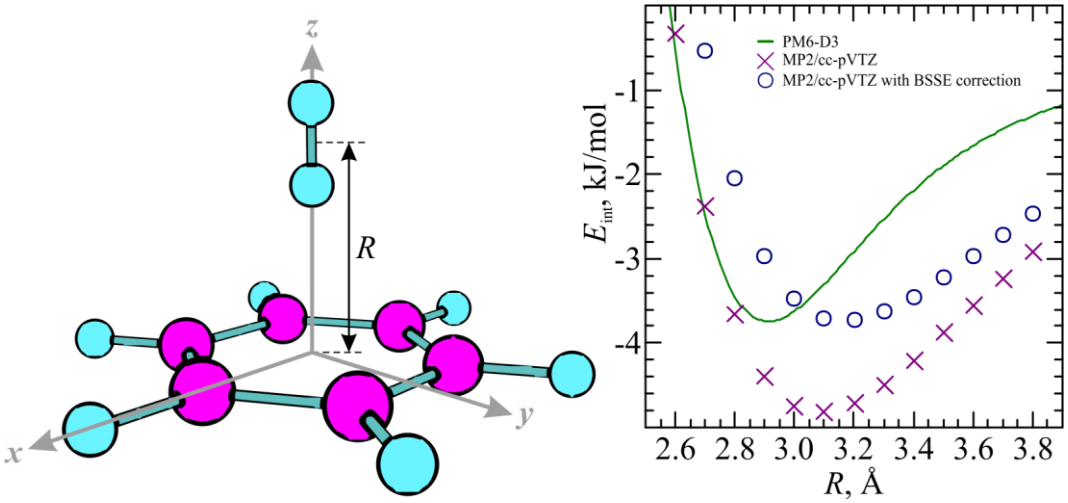

Figure 2 – Benzene and hydrogen molecule in Cartesian coordinate system (left), dependence of the binding energy between them on the distance *R* (right). MP2/cc-pVTZ results are taken from the ref. [42]

As was previously mentioned, the results of MOPAC2016 calculations correspond to 298 K while *ab initio* calculations give zero-temperature values. So, one can reach quite good agreement with BSSE-corrected MP2/cc-pVTZ method if using 100 K (the minimum temperature recommended for consideration by MOPAC2016 developers [49]) values of ΔH_f. Binding energy between hydrogen and coronene molecule is then equal to 6.41 kJ/mol.

3.2. Hydrogen sorption capacity of graphite

The approach proposed for the estimation of hydrogen pressure needed for the reference concentrations of hydrogen inside the schwarzites at given temperatures was first tested using graphite supercell.

This model was previously investigated by *Patchkovskii et al.* with respect to the increasing of interplanar spacing in graphite [42]. Lennard-Jones parameters for dispersion interaction of hydrogen with carbon surface were defined using *ab initio* calculations. Then, the energy of hydrogen molecule was estimated for the given potential and vacuum, and constants of equilibrium between free and adsorbed hydrogen were obtained. The values of pressure needed for the reference H_2 concentration at given temperature were then calculated. In particular, the weight fraction of hydrogen adsorbed in graphite was found to be 5.0-6.5 % when interplanar distance increased up to 8 Å (T = 200 K, P = 5 MPa or T = 250 K, P = 10 MPa).

According to the abovementioned results, 8×8×1 graphite supercell (256 carbon atoms) was used for the test. Different amounts of hydrogen molecules (from 60 to 120 molecules with the step of 10 molecules) were placed inside the structure (see Figure 3). Optimized translation vectors of graphite cell were found to be a=b=19.79 Å, c=16 Å, α=β=90º, γ=120º. Thus, the spacing between graphite layers is 8 Å. This value was fixed during the optimization.

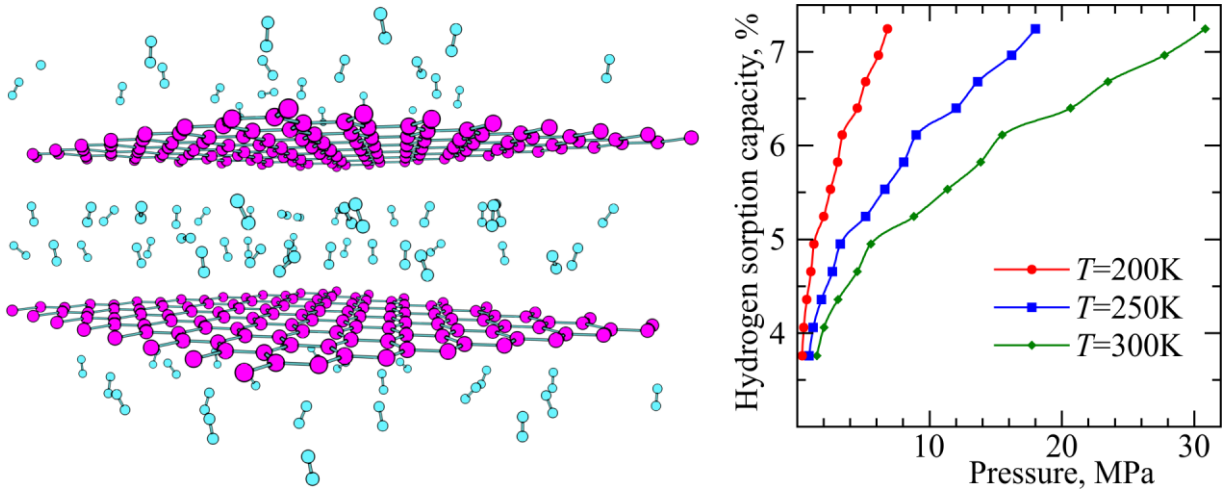

Figure 3 – Graphite supercell containing 85 H_2 molecules (left); molecular hydrogen adsorption isotherms at three different temperatures (right). Graphite interlayer distance is set to 8 Å

It was shown (see Figure 3) that hydrogen weight fraction in graphite reaches 6.61% at 200 K and 5 MPa, slightly exceeding the value previously reported by *Patchkovskii et al.* [42]. However, it decreases down to 6.23% at 250 K and 10 MPa, now lying in the reference range of 5.0-6.5% [42] though being close to its upper limit. Hence, the approach we propose allows one to obtain the results which are in general agreement with the reference data though the sorption capacity can be slightly overestimated by 1-1.5%. The corresponding values of external pressure needed for the reference concentration of hydrogen molecules adsorbed in the model graphite structure at different temperatures can be found in Table S7 [Supplementary Material].

3.3. Hydrogen sorption capacity of D-schwarzites

According to the values of gravimetric density, schwarzites *D*168, *D*224, *D*360 and *D*480 are considerably lightweight materials (see Table 3). Their porous structure provides large accessible surface area (ASA) which is extremely important for molecular hydrogen sorption. The ASA and porosity values were estimated using the approach of «rolling» a probe molecule along the surface [29,30,57]. Hydrogen molecule was treated as the σ diameter sphere with σ = 2.958 Å corresponding to the value of Lennard-Jones parameter. Similarly, carbon atom diameter was chosen to be σ = 3.431 Å. The porosity was found as the volume of schwarzite unit cell accessible for filling by the hydrogen molecules without overlapping divided by the bare volume of the unit cell (see Table 3).

Table 3 – Gravimetric parameters and accessible surface area (ASA) of *D*-schwarzites

Schwarzite	*D*168	*D*224	*D*360	*D*480
Density, kg/m^3	1257	1115	853	745
Porosity	0,42	0,34	0,38	0,41
ASA, m^2/g	1341	1714	2113	2301

According to the values obtained, the weight fraction of H_2 molecules inside *D*168 structure is only 3.26% at 200 K and 5 MPa (see Figure 4) and doesn't increase much at higher pressure (0.8% increase at 10 MPa). Hence, in order to reach the hydrogen capacity comparable to that of graphite, the external pressure of hydrogen should be 10 times larger at the given temperature. *D*168 schwarzite is then not efficient for hydrogen storage.

Similarly, the weight fraction of hydrogen inside *D*224 schwarzite is also considerably low: 4.60%, 3.75% and 3.34% at 200 K, 250 K and 300 K and constant pressure of 10 MPa, respectively. Taking into account the possible overestimation of hydrogen concentration, the actual values can be 1-1.5% lower. These values are in agreement with previously reported data [30]. In particular, ASA value of welded (8,8) and (14,0) carbon nanotubes proposed as the model of carbon foam is close to that of *D*224 (1650 m^2/g) while the hydrogen weight fraction lies in the range of 0.5-3.5% at T = 298 K and P = 10 MPa, depending on the corresponding potential for intermolecular interaction.

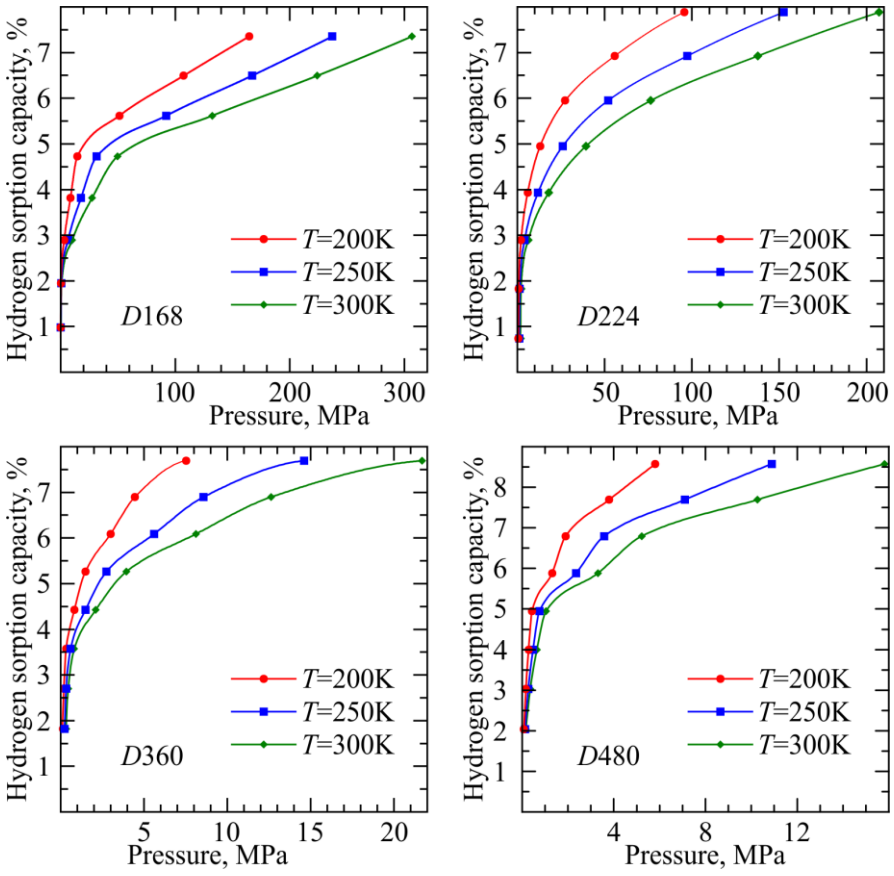

Figure 4 – Isotherms of molecular hydrogen adsorption in *D*-schwarzites at three different temperatures (corresponding values of external pressure needed for the certain concentration of hydrogen inside the structures at different temperatures can be found in Tables S8-S11 [Supplementary Material])

In contrast to that, *D*360 and *D*480 schwarzites are significantly different from former ones in terms of hydrogen adsorption. The weight fraction of H_2 is 5.93% for *D*360 and 7.24% for *D*480 at 250 K and 5 MPa. Moreover, *D*480 sorption capacity reaches 7.65% at 300 K and 10 MPa. According to that, *D*480 sorption characteristics surpass both other schwarzite structures and graphite. It turns out that large ASA is to be responsible for these outstanding characteristics since it visibly increases with increasing of the size of *D*-schwarzite. Along with that, porosity is unlikely to influence the sorption capacity in schwarzite structures. Maximum and minimum values of porosity correspond to *D*168 and *D*224 structures, without any correlation with hydrogen sorption capacity. However, it can still have some effect when comparing carbon nanostructures of different topology.

4. Conclusion

Quantum chemical modeling of *D*-schwarzites as the models for nanoporous carbon and their molecular hydrogen sorption capacity showed that the weight fraction of H_2 inside the structure primarily depends on its size and corresponding value of the accessible surface area. Sorption capacity increases with increase of the number of carbon atoms reaching 7.65% for *D*480 at 300 K and 10 MPa. Keeping in mind the fact of possible overestimation, the actual value can be decreased to 6%. This value is lower than that required by DOE (9%) but the difference can be eliminated. Accessible surface area increases with increase of the schwarzite unit cell. Hence, larger schwarzites should provide larger weight fractions of adsorbed hydrogen. However, it was found that schwarzites' porosity doesn't change much and thus doesn't affect the hydrogen sorption capacity. Besides that, schwarzites can be used as cages for alkaline atoms intercalation (e.g. Li) which was proved to enhance the energy of hydrogen adsorption.

5. Acknowledgements

The work was supported by Ministry of Education and Science of Russia (Russian-Japanese joined project, Agreement 14.613.21.0010, ID RFMEFI61314X0010). The authors are grateful to the Data-Computing Center of Novosibirsk State University for providing the opportunities to use supercomputer.

6. References

1. Ströbel R, Garche J, Moseley PT, Jörissen L, Wolf G. Hydrogen storage by carbon materials. J Power Sources 2006; 159: 781-801.
2. Yürüm Y, Taralp A, Veziroglu TN. Storage of hydrogen in nanostructured carbon materials. Int J Hydrogen Energy 2009; 34: 3784-98.

3. Srivastava M, Kumar M, Singh R, Agrawal UC, Garg MO. Energy-related applications of carbon materials – a review. J Sci Ind Res 2009; 68: 93-6.
4. Lim KL, Kazemian H, Yaakob Z, Daud WRW. Solid-state materials and methods for hydrogen storage: a critical review. Chem Eng Technol 2010; 33: 213-26.
5. Froudakis GE. Hydrogen storage in nanotubes and nanostructures. Mater Today 2011; 14: 324-8.
6. Zollo G, Gala F. Atomistic modeling of gas adsorption in nanocarbons. J Nanomaterials 2012; 2012: 152489.
7. Tozzini V, Pellegrini V. Prospects for hydrogen storage in graphene. Phys Chem Chem Phys 2013; 15: 80-9.
8. Durbin DJ, Malardier-Jugroot C. Review of hydrogen storage techniques for on board vehicle applications. Int J Hydrogen Energy 2013; 38: 14595-617.
9. Cheng HM, Yang QH, Liu C. Hydrogen storage in carbon nanotubes. Carbon 2001; 39: 1447-54.
10. Meregalli V, Parrinello M. Review of theoretical calculations of hydrogen storage in carbon-based materials. Appl Phys A 2001; 72: 143-6.
11. Lamari Darkrim F, Malbrunot P, Tartaglia GP. Review of hydrogen storage by adsorption in carbon nanotubes. Int J Hydrogen Energy 2002; 27: 193-202.
12. Froudakis GE. Hydrogen interaction with carbon nanotubes: a review of ab initio studies. J Phys: Condens Matter 2002; 14: R453-65.
13. Hirscher M, Becher M. Hydrogen storage in carbon nanotubes. J Nanosci Nanotechnol 2003; 3: 3-17.
14. Becher M, Haluska M, Hirscher M, Quintel A, Skakalova V, Dettlaff-Weglikovska U, Chen X, Hulman M, Choi Y, Roth S, Meregalli V, Parrinello M, Ströbel R, Jörissen L, Kappes MM, Fink J, Züttel A, Stepanek I, Bernier P. Hydrogen storage in carbon nanotubes. C R Physique 2003; 4: 1055-62.
15. Oriňáková R, Oriňák A. Recent applications of carbon nanotubes in hydrogen production and storage. Fuel 2011; 90: 312340.
16. Türker L, Erkoç Ş. AM1 treatment of endohedrally hydrogen doped fullerene, $n H_2@C_{60}$. J Mol Struct 2003; 638: 37-40.
17. Dolgonos G. How many hydrogen molecules can be inserted into C_{60}? Comments on the paper 'AM1 treatment of endohedrally hydrogen doped fullerene, $n H_2@C_{60}$' by L. Türker and Ş. Erkoç [J. Mol. Struct. (Theochem) 638 (2003) 37–40]. J Mol Struct 2005; 723: 239-41.
18. Li M, Tang Q, Zhou Z. Recent computational explorations for nanostructured hydrogen storage materials. J Comput Theor Nanosci 2011; 8: 2398-405.

19. Singh AK, Yakobson BI. First principles calculations of H-storage in sorption materials. J Mater Sci 2012; 47: 7356-66.
20. Yildirim T, Ciraci S. Titanium-decorated carbon nanotubes as a potential high-capacity hydrogen storage medium. Phys Rev Lett 2005; 94: 175501.
21. Durgun E, Ciraci S, Zhou W, Yildirim T. Transition-metal-ethylene complexes as high-capacity hydrogen-storage media. Phys Rev Lett 2006; 97: 226102.
22. Han SS, Goddard III WA. Lithium-doped metal-organic frameworks for reversible H_2 storage at ambient temperature. J Am Chem Soc 2007; 129: 8422-3.
23. Huang L, Liu YC, Gubbins KE, Nardelli MB. Ti-decorated C_{60} as catalyst for hydrogen generation and storage. Appl Phys Lett 2010; 96: 063111.
24. Krasnov PO, Ding F, Singh AK, Yakobson BI. Clustering of Sc on SWNT and reduction of hydrogen uptake: ab-initio all-electron calculations. J Phys Chem C 2007; 111: 17977-80.
25. Kuzubov AA, Krasnov PO, Kozhevnikova TA, Popov MN. Calculation of the energy of binding of titanium and scandium complexes to the surface of carbon nanotubes. Rus J Phys Chem B 2009; 3: 679-83.
26. Kuzubov AA, Krasnov PO, Kozhevnikova TA, Popov MN, Artyushenko PV. Peculiarities of the decoration of carbon nanotubes with transition metal atoms. Rus J Phys Chem B 2011; 5: 163-7.
27. Candelaria SL, Shao Y, Zhou W, Li X, Xiao J, Zhang JG, Wang Y, Liu J, Li J, Gao G. Nanostructured carbon for energy storage and conversion. Nano Energy 2012; 1: 195-220.
28. Martínez-Mesa A, Yurchenko SN, Patchkovskii S, Heine T, Seifert G. Influence of quantum effects on the physicsorption of molecular hydrogen in model carbon foam. J Chem Phys 2011; 135: 214701.
29. Kumar KV, Salih A, Lu L, Müller EA, Rodríguez-Reinoso F. Molecular simulation of hydrogen physisorption and chemisorption in nanoporous carbon structures. Adsorpt Sci Technol 2011; 29: 799-817.
30. Singh AK, Lu J, Aga RS, Yakobson BI. Hydrogen storage capacity of carbon-foams: grand canonical Monte Carlo simulations. J Phys Chem C 2011; 115: 2476.
31. Goncharov A, Guglya A, Melnikova E. On the feasibility of developing hydrogen storage capable of adsorption hydrogen both in its molecular and atomic states. Int J Hydrogen Energy 2012; 37: 18061-73.
32. Martínez-Mesa A, Zhechkov L, Yurchenko SN, Heine T, Seifert G, Rubayo-Soneira J. Hydrogen physisorption on carbon foams upon inclusion of many-body and quantum delocalization effects. J Phys Chem C 2012; 116: 19543-53.
33. Nishihara H, Kyotani T. Templated nanocarbons for energy storage. Adv Mater 2012; 24: 4473-98.

34. Alonso JA, Cabria I, López MJ. Simulation of hydrogen storage in porous carbons. J Mater Res 2013; 28: 589-604.
35. Lyth SM, Shao H, Liu J, Sasaki K, Akiba E. Hydrogen adsorption on graphene foam synthesized by combustion of sodium ethoxide. Int J Hydrogen Energy 2014; 39: 376-80.
36. Blinc R, Arčon D, Umek P, Apih T, Milia F, Rode AV. Carbon nanofoam as a potential hydrogen storage material. Phys Stat Sol (B) 2007; 244: 4308-10.
37. Ding F, Lin Y, Krasnov PO, Yakobson BI. Nanotube-derived carbon foam for hydrogen sorption. J Chem Phys 2007; 127: 164703.
38. Hynek S, Fuller W, Bentley J. Hydrogen storage by carbon sorption. Int J Hydrogen Energy 1997; 22: 601-10.
39. Satyapal S, Petrovic J, Read C, Thomas G, Ordaz G. The U.S. Department of Energy's National Hydrogen Storage Project: Progress towards meeting hydrogen-powered vehicle requirements. Catal Today 2007; 120: 246-56.
40. Dillon AC, Jones KM, Bekkedahl TA, Kiang CH, Bethune DS, Heben MJ. Storage of hydrogen in single-walled carbon nanotubes. Nature 1997; 386: 377-9.
41. Hirscher M, Becher M, Haluska M, Quintel A, Skakalova V, Choi YM, Dettlaff-Weglikowska U, Roth S, Stepanek I, Bernier P, Leonhardt A, Fink J. Hydrogen storage in carbon nanostructures. J Alloys Compd 2002; 330-332: 654-8.
42. Patchkovskii S, Tse JS, Yurchenko SN, Zhechkov L, Heine T, Seifert G. Graphene nanostructures as tunable storage media for molecular hydrogen. PNAS 2005; 102: 10439-44.
43. Aga RS, Fu CL, Krčmar M, Morris JR. Theoretical investigation of the effect of graphite interlayer spacing on hydrogen absorption. Phys Rev B 2007; 76: 165404.
44. Vanderbilt D, Tersoff J. Negative-curvature fullerene analog of C_{60}. Phys Rev Lett 1992; 68: 511-3.
45. Ching WY, Huang MZ, Xu Y. Electronic and optical properties of the Vanderbilt-Tersoff model of negative-curvature fullerene. Phys Rev B 1992; 46: 9910-2.
46. Townsend SJ, Lenosky TJ, Muller DA, Nichols CS, Elser V. Negatively curved graphical sheet model of amorphous carbon. Phys Rev Lett 1992; 69: 921-4.
47. Huang MZ, Ching WY, Lenosky T. Electronic properties of negative-curvature periodic carbon surface. Phys Rev B 1993; 47: 1593-606.
48. Stewart JJP. Optimization of parameters for semiempirical methods V: Modification of NDDO approximations and application to 70 elements. J Mol Model 2007; 13: 1173-213.
49. MOPAC2016, J.J.P. Stewart, Stewart Computational Chemistry, Colorado Springs, CO, USA, http://OpenMOPAC.net; 2016 [assessed 12.01.17].

50. Grimme S, Antony J, Ehrlich S, Krieg H. A consistent and accurate ab initio parametrization of density functional dispersion correction (DFT-D) for the 94 elements H-Pu. J Chem Phys 2010; 132: 154104.
51. Stokes HT, Hatch DM. FINDSYM: program for identifying the space-group symmetry of a crystal. J Appl Cryst 2005; 38: 237-8.
52. Dewar MJS, Ford GP. Ground states of molecules. 44. MINDO/3 calculations of absolute heat capacities and entropies of molecules without internal rotations. J Am Chem Soc 1977; 99: 7822-9.
53. Shaw HR, Wones DR. Fugacity coefficients for hydrogen gas between 0º and 1000ºC, for pressures to 3000 atm. Am J Sci 1964; 262: 918-29.
54. Deming WE, Shupe LE. Some physical properties of compressed gases, III. Hydrogen. Phys Rev 1932; 40: 848-59.
55. Lide DR, editor-in-chief. CRC Handbook of Chemistry and Physics, 84th edition, CRC Press; 2003; p. 9-19.
56. Heine T, Zhechkov L, Seifert G. Hydrogen storage by physisorption on nanostructured graphite platelets. Phys Chem Chem Phys 2004; 6: 980-4.
57. Frost H, Düren T, Snurr RQ. Effects of Surface Area, Free Volume, and Heat of Adsorption on Hydrogen Uptake in Metal-Organic Frameworks. J Phys Chem B 2006; 110: 9565-9570.